Expression of the "4.2 ka event" in the southern Rocky Mountains, USA

David T. Liefert[1], Bryan N. Shuman[1]

1) Department of Geology and Geophysics, University of Wyoming, Laramie, WY 82070, USA

Correspondence to: David T. Liefert (dliefert@openspace.org)

Abstract

The use of the climatic anomaly known as the "4.2 ka event" as the stratigraphic division between the mid- and late Holocene has prompted debate over its impact, geographic pattern, and significance. The anomaly has primarily been described as abrupt drying in the Northern Hemisphere at ca. 4 ka (ka, thousands of years before present), but evidence of the hydroclimate change is inconsistent among sites, both globally and within North America. Climate records from the southern Rocky Mountains demonstrate the challenge with diagnosing the extent and severity of the anomaly. Dune-field chronologies and a pollen record in southeast Wyoming reveal several centuries of low moisture at around 4.2 ka and prominent low stands in lakes in Colorado suggest the drought was unique amid Holocene variability, but detailed carbonate oxygen isotope ($\delta^{18}O_{carb}$) records from Colorado do not record drought at the same time. We find new evidence from $\delta^{18}O_{carb}$ in a small mountain lake in southeast Wyoming of an abrupt reduction in effective moisture or snowpack from approximately 4.2–4 ka, which coincides in time with the other evidence of regional drying from the southern Rocky Mountains and the western Great Plains. We find that the $\delta^{18}O_{carb}$ in our record may reflect cool-season inputs into the lake, which do not appear to track the strong enrichment of heavy oxygen by evaporation during summer months today. The modern relationship differs from some widely applied conceptual models of lake-isotope systems and may indicate reduced winter precipitation rather than enhanced evaporation at ca. 4.2 ka. Inconsistencies among the North American records, particularly in $\delta^{18}O_{carb}$ trends, thus show that site-specific factors can prevent identification of the patterns of multi-century drought. However, the prominence of the drought at ca. 4 ka among a growing number of sites in the North American interior suggests it was a regionally substantial climate event amid other Holocene variability.

1. Introduction

Rapid climate changes are well documented in the late Pleistocene and early Holocene, such as during the Younger Dryas chronozone (ca. 12.9-11.7 ka, thousands of years before present) and at 8.2 ka (Alley et al., 1997; Clark et al., 1999; Von Grafenstein et al., 1998), but mid- to late-Holocene changes are less well understood (Wanner et al., 2008, 2011). One potential abrupt change during this time, a multi-century climatic anomaly known as the "4.2 ka event," has been used as the benchmark for the stratigraphic division between the mid- and late Holocene (Walker et al., 2019). Consequently, the 4.2 ka event has become a topic of scrutiny with debate over its impact, geographic pattern, and significance (Bradley & Bakke, 2019; Weiss, 2016, 2019). The ostensibly global event has primarily been described as a dry episode at low and mid-latitudes (Booth et al., 2005; Nakamura et al., 2016; Di Rita & Magri, 2019; Scuderi et al., 2019; Xiao et al., 2018). However, some regions show increased precipitation (Huang et al., 2011; Railsback et al., 2018) or no change (Roland et al., 2014), as is consistent with spatial variation expected from climate variability that shifts atmospheric waves and dynamics.

The 4.2 ka event has been widely examined, but its cause and significance amid other millennial-to-centennial climate variability during the Holocene remain unknown. Processes that may have been involved in the event included changes in solar irradiance (Wang et al., 2005), centennial-scale atmospheric circulations (Deininger et al., 2017), and latitudinal shifts in the Intertropical Convergence Zone (Tan et al., 2008). Recent model simulations have produced similar patterns of extended drought in the northern hemisphere without external forcings such as insolation changes or volcanism (Yan & Liu, 2019), and others confirm that multi-decadal megadroughts can arise through internal climate variability without changes in boundary

71 conditions (Ault et al., 2018). Internal climate dynamics and feedbacks could also interact with
72 stochastic variability and external forcing to produce such events without consistent or linear
73 relationships to the forcing; forcing may only have a modest probability of triggering rapid
74 climate changes (Renssen et al., 2006). Less clear is how unusual or frequent prolonged
75 'megadroughts' may be within the Holocene across different regions.
76 That such droughts can occur stochastically indicates the 4.2 ka event could be an
77 example of typical late-Holocene climate variability at multi-century time scales (Shuman &
78 Burrell, 2017), even if the event was exceptional within the spectrum of Holocene variability in
79 some regions. For example, the event is recorded in the northeastern United States as one
80 drought period within a series of Holocene wetting and drying events (Newby et al., 2014;
81 Shuman et al., 2019; Shuman & Burrell, 2017); evidence for a major hydroclimate change at ca.
82 4 ka has been growing in the North American midcontinent (Booth et al., 2005; Carter et al.,
83 2018; Dean, 1997; Denniston et al., 1992; Halfen & Johnson, 2013; Jiménez-Moreno et al.,
84 2019). However, the event's significance or uniqueness has been difficult to verify in this region
85 because few sites document the anomaly compared to other regions of the mid-latitudes globally
86 (Ran & Chen, 2019; Zhang et al., 2018).
87 Records from the southern Rocky Mountains of North America demonstrate the
88 challenge. In the mid-latitude Rocky Mountains, only dune-field chronology and pollen records
89 have been explicitly interpreted to show the 4.2 ka event while other record types, such as stable
90 isotopes, have not. Initial recognition in North America derived from the timing of the
91 reactivation of the Ferris, Seminoe, and Casper Dune Fields in southeast Wyoming (Fig. 1, Table
92 1; Booth et al., 2005; Halfen et al., 2010; Stokes & Gaylord, 1993), but the extent of the drought
93 has been unclear because other dune-field chronologies in the adjacent western Great Plains do

not clearly document the drought (Dean, 1997; Halfen & Johnson, 2013; Mason et al., 1997). More recently, Carter et al. (2013, 2017a, 2018) used fossil pollen from Long Lake in the Medicine Bow Mountains, south of the Wyoming dune fields (Fig. 1, Table 1), to identify a 150-year interval of increased temperature and decreased precipitation centered at 4.2 ka. The inferred precipitation reductions were largest in springtime (Carter et al., 2018), when snowfall in the southern Rocky Mountains is highest today (Mock, 1996). Consistent with this interpretation, stratigraphic evidence of lake-level changes in Colorado and Wyoming lakes could indicate that low-water phases at ca. 4.2 ka were one of the most prominent hydrologic changes during the Holocene (Jiménez-Moreno et al., 2019; Shuman et al., 2009; Shuman et al., 2014, 2015). The drying event stands out as one of the only multi-centennial features in a summary of low lakes in the Rocky Mountains during the late-Quaternary (Shuman and Serravezza 2017).

By contrast, the 4.2 ka event does not appear in stable oxygen isotope records from lakes in the same region, such as detailed carbonate-$\delta^{18}O$ ($\delta^{18}O_{carb}$) records from Bison and Yellow lakes, Colorado (Fig. 1, Table 1; Anderson, 2011, 2012). Widely applied conceptual models of lake-isotope systems indicate that climate-driven changes in the stable isotope composition of lake water become archived in lacustrine carbonates (e.g., Anderson et al., 2016; Leng & Marshall, 2004; Talbot, 1990). According to such models, site-specific hydrologic controls on isotope budgets and the timing of carbonate formation should also play an important role in how the 4.2 ka event was recorded, but the isotopic response should vary predictably by hydrologic setting: long lake-water residence times and high evaporation cause hydrologically closed lakes (i.e., terminal basins) to record shifts in effective moisture (precipitation – evaporation) because endogenic carbonates typically precipitate in evaporated, ^{18}O-rich water during the warm

summer months. Drought could drive a positive change in the isotope composition of lake water within such a lake-isotope system by both increasing evaporation and changing seasonal precipitation, such as by reducing snowpack. In hydrologically open lakes with short residence times, the continual replacement of evaporated water creates isotopic sensitivity primarily to the seasonal balance of precipitation without a strong evaporation effect. In either model, $\delta^{18}O_{carb}$ tracks the isotope composition of lake water and its response to climate changes.

Many lakes fall somewhere between fully hydrologically open and closed and additional site-specific influences may also override such expectations. Consequently, not all stable oxygen isotope records from lakes may have been sensitive to the specific climate variables that changed at 4.2 ka. Modern lake-water isotopic measurements (Fig. 2) can help to identify the relative influences of different controls on the magnitude and range of lake-water $\delta^{18}O$, such as groundwater fluxes and other seasonal dynamics that modify lake-water residence times. We examine how the seasonality of carbonate formation could cause the relationships of lake-water $\delta^{18}O$ to $^{18}O_{carb}$ to differ from the modern patterns observable in lakes today.

Here we present a new $\delta^{18}O_{carb}$ record from Highway 130 Lake (HL) in southeast Wyoming near where other Holocene paleohydrological and paleoecological records have been developed (Fig. 1, Table 1; Mensing et al., 2012; Minckley et al., 2012; Brunelle et al., 2013). HL is an intermittently closed subalpine lake in the Medicine Bow Mountains, within 20 km of Long Lake where fossil pollen indicates a prolonged ‘megadrought’ at 4.2 ka (Carter et al., 2018). The lake is also <60 km from Upper Big Creek Lake, Colorado, where a prominent paleoshoreline detected in geophysical surveys and cores indicates low water after 4.7 ka (Fig. 1, Table 1; Shuman et al., 2015). Previous work at HL indicates a strong influence of evaporation on the lake and the stable isotope composition of its water, which we compare with Bison and

Yellow lakes in Colorado (Fig. 2; Liefert et al., 2018). We discuss how dissimilarities in $\delta^{18}O_{carb}$ among lakes, possibly driven by non-climatic factors, could complicate interpretations of the patterns of past hydroclimate changes including megadroughts and Holocene trends. Together these outcomes may clarify the timescales on which drought operates within a critical headwater area of North America, but also confirm that interpretations of past hydroclimate changes using $\delta^{18}O_{carb}$ may depend heavily on site-specific dynamics.

Table 1. Changes at ca. 4.2 ka inferred from North American climate records nearby Highway 130 Lake, southeast Wyoming, USA.

Study	Site Name	Region	Climate Record	Change at ca. 4.2 ka
Carter et al., 2013; 2017a	Long Lake	Southeast Wyoming, USA	Fossil pollen	Warming/drying
Halfen et al., 2010	Casper Dune Field	Southeast Wyoming, USA	Dune-field chronology	Drying
Stokes & Gaylord, 1993	Ferris/Seminoe Dune Field	Southeast Wyoming, USA	Dune-field chronology	Drying
Anderson, 2011	Bison Lake	East-central Colorado, USA	Lacustrine carbonate $\delta^{18}O$	No prominent change
Anderson, 2012	Yellow Lake	East-central Colorado, USA	Lacustrine carbonate $\delta^{18}O$	No prominent change
Shuman et al., 2015	Upper Big Creek Lake	North-central Colorado, USA	Sedimentary lake-level record	Drying
Shuman et al., 2009a	Little Molas Lake	Central Colorado, USA	Sedimentary lake-level record	Drying
Shuman et al., 2014	Emerald Lake	Central Colorado, USA	Sedimentary lake-level record	Drying

2. **Site description**

HL (41°21’05” N, 106°15’50” W; 3,199 m a.s.l. (above sea level)) fills a shallow depression in the uneven terrain covering the Libby Creek watershed (12 km^2 surface area) in the Snowy Range, a southwest trending subsection of the Medicine Bow Mountains in southeast Wyoming (Fig. 1). Around HL, subalpine coniferous forests interspersed with open meadows grow on thin glaciated soils and tills between the frequent outcroppings of the underlying siliceous metadolomite (Houston & Karlstrom, 1992; Musselman et al., 1992). Southeast Wyoming has a semi-arid climate, but the Medicine Bow Mountains receive about 1,000 mm of precipitation each year, with approximately 70% of annual totals falling as snow from October to June (Mock, 1996). Local average wind speeds are high (~5 m/s) and minimum winter and maximum summer temperatures typically reach -23°C and 21°C, respectively (SNOTEL station ID 367).

The surface watershed around HL occupies ~0.45 km^2, while the lake has a surface area of ~0.02 km^2, a maximum (spring) water depth of ~200 cm, and declines in water level by ~30 cm from July to late October (Liefert et al., 2018). Ice covers HL from approximately October to May and stream connections shut off in June following spring flooding. Measurements reveal no thermal stratification because of the shallow water depth, flat-bottom bathymetry, and high average wind speeds, which promote mixing throughout the water column (Bello & Smith, 1990; Stewart & Rouse, 1976). Liefert et al. (2018) found that evaporation could account for as much as 83% of the seasonal water loss at HL, though the stable water level and temperature compared to nearby lakes of similar size and depth indicates shallow groundwater flow-through driven by seasonal precipitation and infiltration (Rautio & Korkka-Niemi, 2011; Rosenberry & LaBaugh, 2008).

174

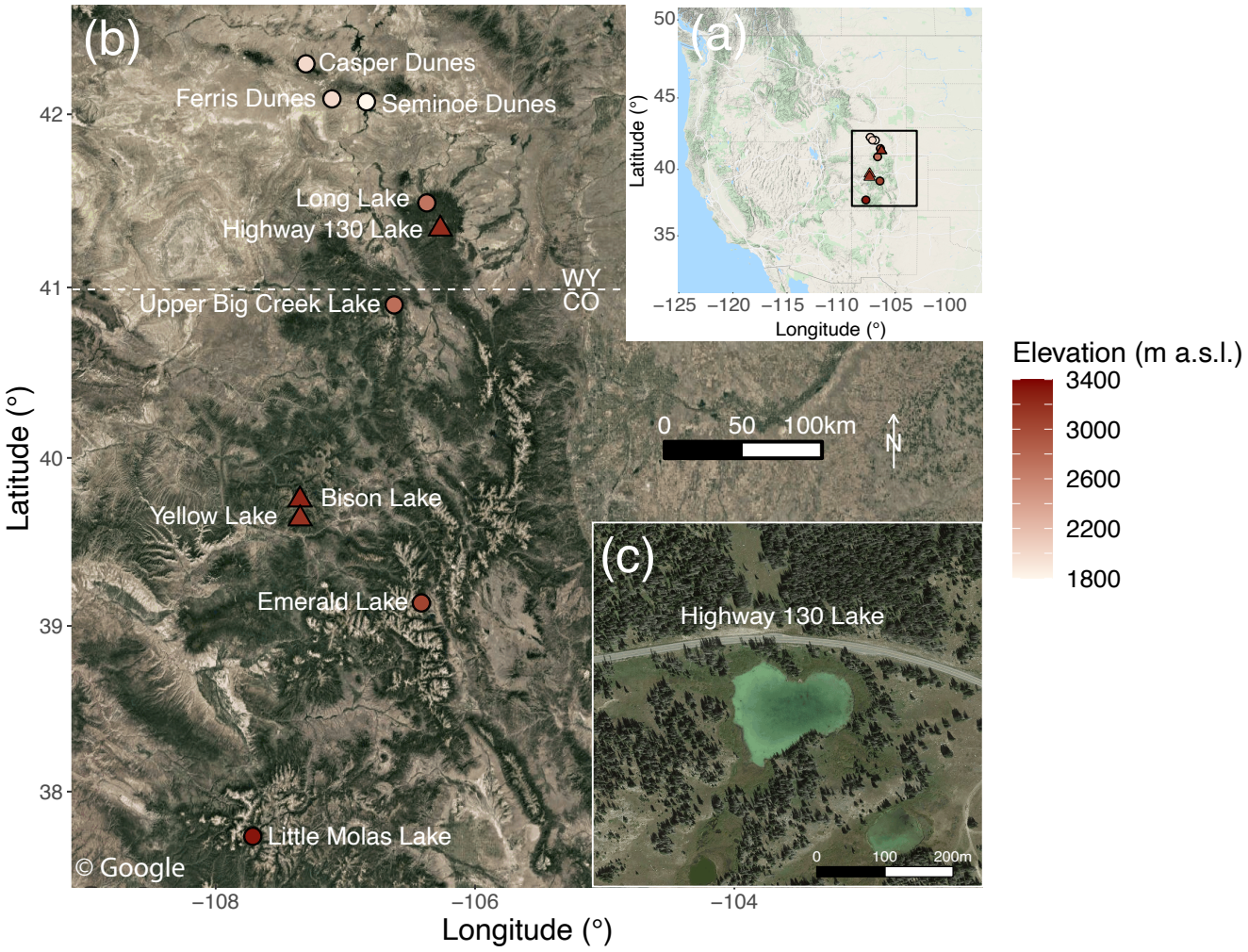

175

Figure 1. Locations of study site and related climate records. (**a**), Highway 130 Lake (triangle; this study) and related carbonate (triangles), dune-field chronology, pollen, and lake-level records (circles) lie within the southern Rocky Mountains, a critical headwater area in the western United States that contributes snowmelt to the Colorado and North Platte Rivers. (**b**), Study site locations in the Colorado Front Range and Medicine Bow Mountains, southeast Wyoming. (**c**), Highway 130 Lake lies within the Snowy Range, a subsection of the Medicine Bow Mountains. Google images (© Google Maps 2021) were acquired using the ggmap package in R (Kahle & Wickham, 2013).

3. **Methods**

To measure the modern oxygen and hydrogen isotope compositions of the lake water ($\delta^{18}O$ and δD, respectively), temperature, and specific conductance, water samples were collected at approximately biweekly intervals from June to October in each year from 2015–2017. Additional samples of snowfall, snowpack, rain, and groundwater (from springs and wells) were collected episodically from 2015–2017 to measure the range in water isotope values of the watershed's hydrologic components. Isotopic ratios of all water samples were measured at the University of Wyoming Stable Isotope Facility using a Picarro L2130-I Cavity Ring Down Spectrometer and specific conductance was measured using a YSI Multiparameter Water Quality Meter. We report $\delta^{18}O$ and δD in the per mil (‰) notation relative to Vienna Standard Mean Ocean Water (VSMOW). We acquired meteorological data from SNOTEL stations near HL at Brooklyn Lake, Wyoming (ID 367; 3,121 m a.s.l.; 41.36 °N, -106.23 °W), and at Bison Lake, Colorado (ID 345; 3,316 m a.s.l.; 39.76 °N, -107.36 °W), to compare the modern ratios of snow/rain that control the seasonal balance of precipitation at the lakes.

In October 2016 we installed a pressure transducer (Onset HOBO U20 Level Data Logger) to measure the water level and temperature of HL at 30-min intervals; freezing conditions required that we secure the transducer to the lakebed inside a bladder filled with antifreeze. To compensate for barometric pressure changes we adjusted the transducer data using pressure measurements from the nearby Glacier Lakes Ecosystem Experiments Site Brooklyn Tower Ameriflux site (GLEES Tower; US-GLE: https://ameriflux.lbl.gov/sites/siteinfo/US-GLE; 41°21'57" N, 106°14'23" W; 3,191 m a.s.l.). In late January 2017, we installed a conductivity data logger (Onset HOBO U24 Conductivity Data Logger) at the same location and water depth as the pressure transducer to measure the range in conductivity (converted to specific

conductance at 25 °C) at 30-min intervals of the unfrozen water underlying the ice cover to examine the seasonal patterns of water chemistry that influence carbonate formation.

On the same day in January 2017, we collected a 70-mm diameter sediment core with a modified Livingston piston corer from the center of HL where the combined water and ice depth reached approximately 90 cm; we used this depth to calibrate the pressure transducer. The organic and carbonate content of contiguous 1-cm intervals of the sediment core were measured by weighing the residual sediment after burning the samples at 550 and 1000 °C, respectively. After the 550 °C burn removed organic matter, we isolated one-cm^3 sub-samples from each interval for isotopic analysis; $\delta^{18}O_{carb}$ of samples burned were within the range of instrument uncertainty (± 0.2‰) as those with organic removal using oxidizing agents (typically bleach), indicating no additional fractionation. Each sub-sample was sieved using a 63-μm mesh to isolate the fine fraction to be used for isotopic analysis using a Thermo Gasbench coupled to a Thermo Delta Plus XL isotope ratio mass spectrometer at the University of Wyoming Stable Isotope Facility. X-ray powder diffraction (XRD) confirmed that the samples contained only microcrystalline calcite. We assume the calcite is predominantly autochthonous because the underlying metadolomite likely provides the Ca ions needed for carbonate formation (if the lacustrine carbonates were clastic deposits from metadolomite then its erosion should deposit more dolomite than calcite) and evidence of biogenic calcite within the core is rare (ostracod tests were present in less than 10 of the 300 samples). We report $\delta^{18}O_{carb}$ in the per mil (‰) notation relative to the Vienna Pee Dee Belemnite (VPDB) standard. To calculate the temperature-dependent fractionation for calcite formation and convert from VSMOW to VPDB, we use equations from Leng and Marshall (2004).

We isolated sedimentary charcoal (>125 μm) from the sediment core for radiocarbon analyses to estimate sedimentation rates. Radiocarbon samples were analyzed at the University of California Irvine Keck Carbon Cycle facility. We calibrated the radiocarbon chronology to calendar years using intcal13 (Reimer et al., 2013) and generated the age-depth model and uncertainties using Bchron (Parnell et al., 2008) and geoChronR (McKay et al., 2021).

4. **Results**

4.1 *Modern water-chemistry and level measurements*

Lake-water $\delta^{18}O$ and δD in HL increased during the ice-free season from -17.8‰ and -132‰ (sampled in late June) to -10.8‰ and -94.2‰ (sampled in late October), respectively (black circles, Fig. 2). The slope of the line tracing the seasonal range in HL's lake-water isotopes (thick black line, Fig. 2) traces the local evaporation line (LEL) defined by samples from lakes in the Colorado Front Range (red dashed line, Fig. 2; Henderson & Shuman, 2009). Several consecutive years of measurements reveal that water isotope values at HL are consistent from year to year. The LEL's deviation from both the global meteoric water line (GMWL; Fig. 2) and isotope composition of the hydrologic inputs (open symbols, Fig. 2) indicates a strong evaporative influence. $\delta^{18}O$ and δD values at HL also indicate stronger fractionation by evaporation compared to representative warm-season isotope compositions measured at Bison and Yellow lakes from June–September around 2010 (thick purple and yellow lines, Fig. 2; Anderson, 2011, 2012), which remained closer to the composition of meteoric waters. Longer lake-water residence time and higher evaporation in HL thus appear to produce a greater range of warm-season isotope compositions compared to Bison and Yellow Lakes.

243 The different lake-water-$\delta^{18}O$ values among the lakes contrasts with their similar
244 seasonal precipitation patterns. The modern ratio of snow/rain, which can determine the mean
245 precipitation and lake-water $\delta^{18}O$, is comparable in the watersheds of HL and Bison Lake when
246 averaged from 1980–2019 (inset plot, Fig. 2). Other modern differences among the lakes, which
247 all have surface areas of < 0.1 km^2, include that the maximum water depth of HL is several
248 meters shallower than Bison and Yellow Lakes (Anderson, 2012) and that the summer lake-
249 water temperatures in HL typically range from 8–12 °C, which is cooler than the epilimnion at
250 Yellow Lake (Anderson, 2012). HL is also several degrees cooler than nearby lakes also without
251 thermal stratification (Liefert et al., 2018).
252 Continuous measurements of specific conductance began in early February when the
253 combined water and ice depth reached approximately 90 cm (Fig. 3). Specific conductance
254 increased from 700 μS/cm to 1,115 μS/cm by early April while the lake surface was frozen. The
255 specific conductance fell below 500 μS/cm as the lake flooded with snowmelt in early May.
256 Specific conductance ranged from 250–300 μS/cm after the conductivity data logger was
257 removed in late June and before the lake froze over in the fall, and the water depth stayed
258 between 100–150 cm, which was low compared to previous years (Liefert et al., 2018).
259

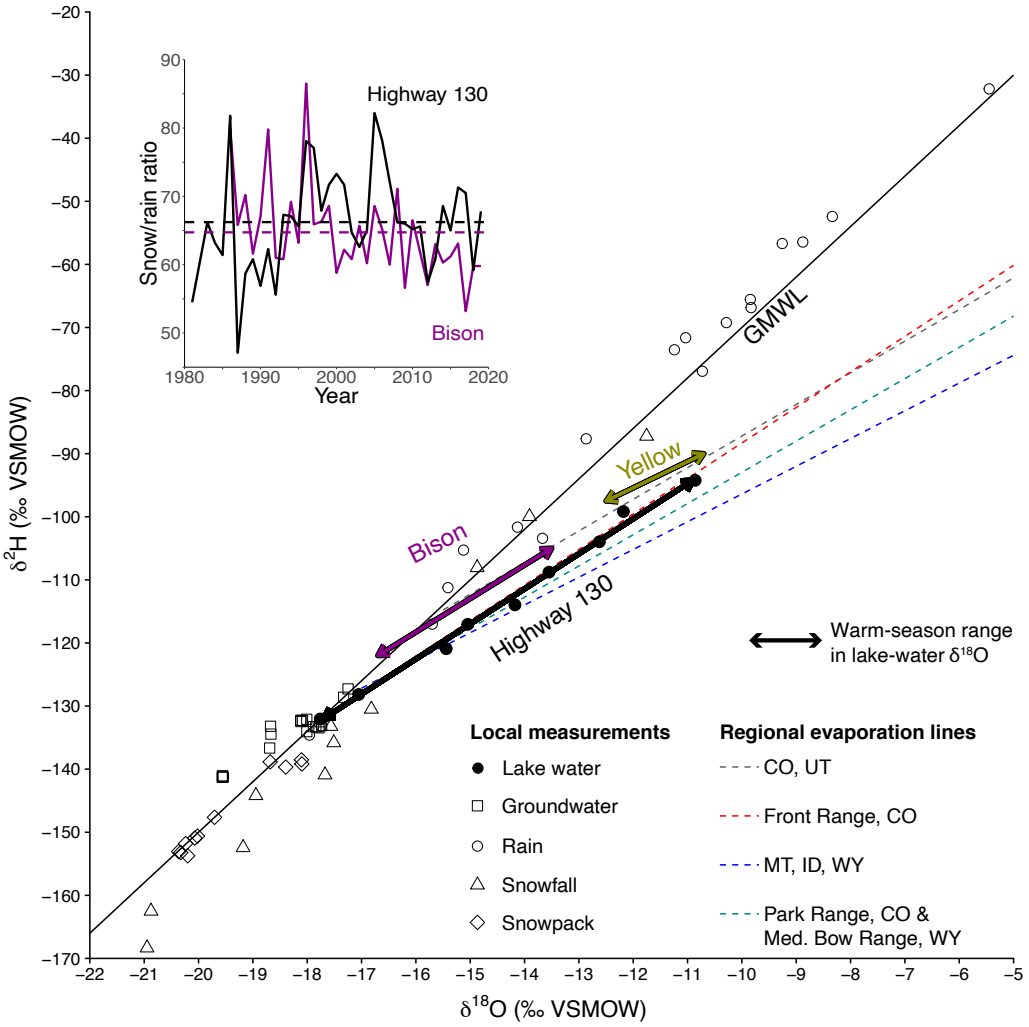

Figure 2. Modern measurements of $\delta^{18}O$ and δD. Samples from the study watershed shown here were collected throughout 2017. Regional evaporation lines (dashed lines; Henderson & Shuman, 2009; Anderson et al., 2016) intersect the global meteoric water line and represent the linear regression of lake-water isotope compositions in a region. Isotopic measurements from the study watershed (open symbols) show the range in isotope compositions of hydrologic inputs to Highway 130 Lake from the watershed. Arrows represent the range in modern $\delta^{18}O$ and δD values of Highway 130 Lake (black), Bison Lake (purple; Anderson, 2011), and Yellow Lake (yellow; Anderson, 2012) throughout the ice-free season, and black dots show the individual measurements at Highway 130 Lake. The inset plot shows the modern annual ratio of snow/rain for the SNOTEL stations nearest Highway 130 Lake (black line) and Bison Lake (purple line) and the dashed lines show the means.

260

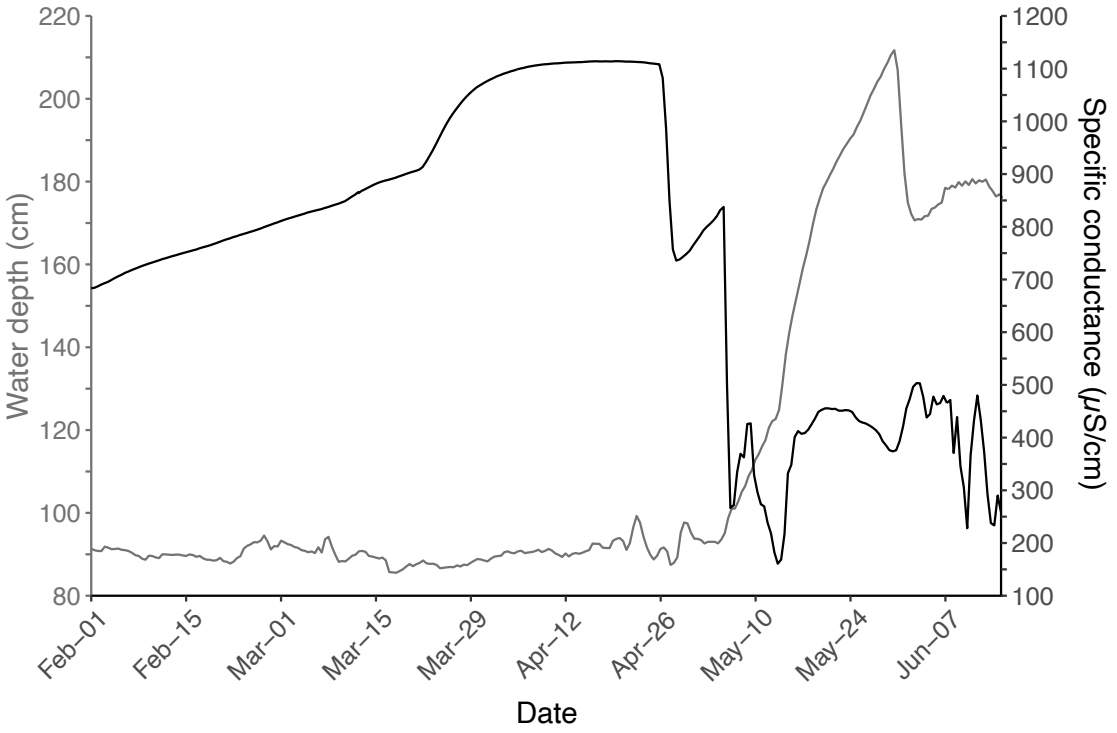

Figure 3. Measurements of water depth (gray line) and specific conductance (black line) at Highway 130 Lake in 2017.

261

262

263 **4.2** ***Sediment characteristics***

264 The 333-cm core from HL extends to at least the early Holocene and contains
265 predominantly carbonate sediment underlain by silicate clays (Fig. 4). The upper 303 cm
266 contains from 5–55% organics and 5–90% carbonate; the core above the basal 30 cm has a mean
267 carbonate content of 65%. In the basal unit, the carbonate content drops below 5%, which was
268 too low for isotopic analysis. The age-depth model (black line with 2-sigma gray uncertainty
269 band, Fig. 4, Table 2) reveals average net sediment accumulation rates of 18 cm/kyr (thousand
270 years) from 11.7–4.4 ka and 45.5 cm/kyr from 4.4 ka to present. High rates of net sedimentation

correspond with intervals of high carbonate flux into the lake, indicating that authigenic carbonate production may largely control sedimentation rates. The carbonate content and carbonate flux, representing the mass of carbonates deposited per unit area per year, increased simultaneously with the sedimentation rate at 4.4 ka (Fig. 4), but the percent carbonate content subsequently declined until 4.0 ka. The radiocarbon age at 119-cm depth (3.072 ± 0.03 ka) has an age similar to the date at 67-cm depth (3.031 ± 0.02 ka), which may indicate a reworked upper age (black dots in Fig. 4). However, high total sediment and carbonate accumulation rates are inferred even if the upper age was excluded from the age-depth model.

Table 2. Calibrated radiocarbon ages used for the age-depth model.

Lake	Core	Depth (cm)	Material	Lab number	Age (^{14}C yr BP)	Uncertainty (1 σ,^{14}C yr BP)	Calibrated age ranges (1 σ, cal yr BP)		
							Median	Maximum	Minimum
Highway 130 Lake	2A	18	Charcoal	UCIAMS-194167	850	30	748	783	726
		67	Charcoal	UCIAMS-194168	2,900	20	3,033	3,070	2,996
	2B	119-121	Charcoal	UCIAMS-194169	2,925	15	3,073	3,144	3,004
		154-156	Charcoal	UCIAMS-194170	3,660	35	3,986	4,081	3,921
		193-195	Charcoal	UCIAMS-194171	3,840	20	4,241	4,290	4,157
		204	Charcoal	UCIAMS-194172	3,965	20	4,438	4,508	4,412
		239	Charcoal	UCIAMS-194173	6,210	60	7,096	7,132	7,007
		302	Charcoal	UCIAMS-194174	9,580	25	10,927	11,074	10,781

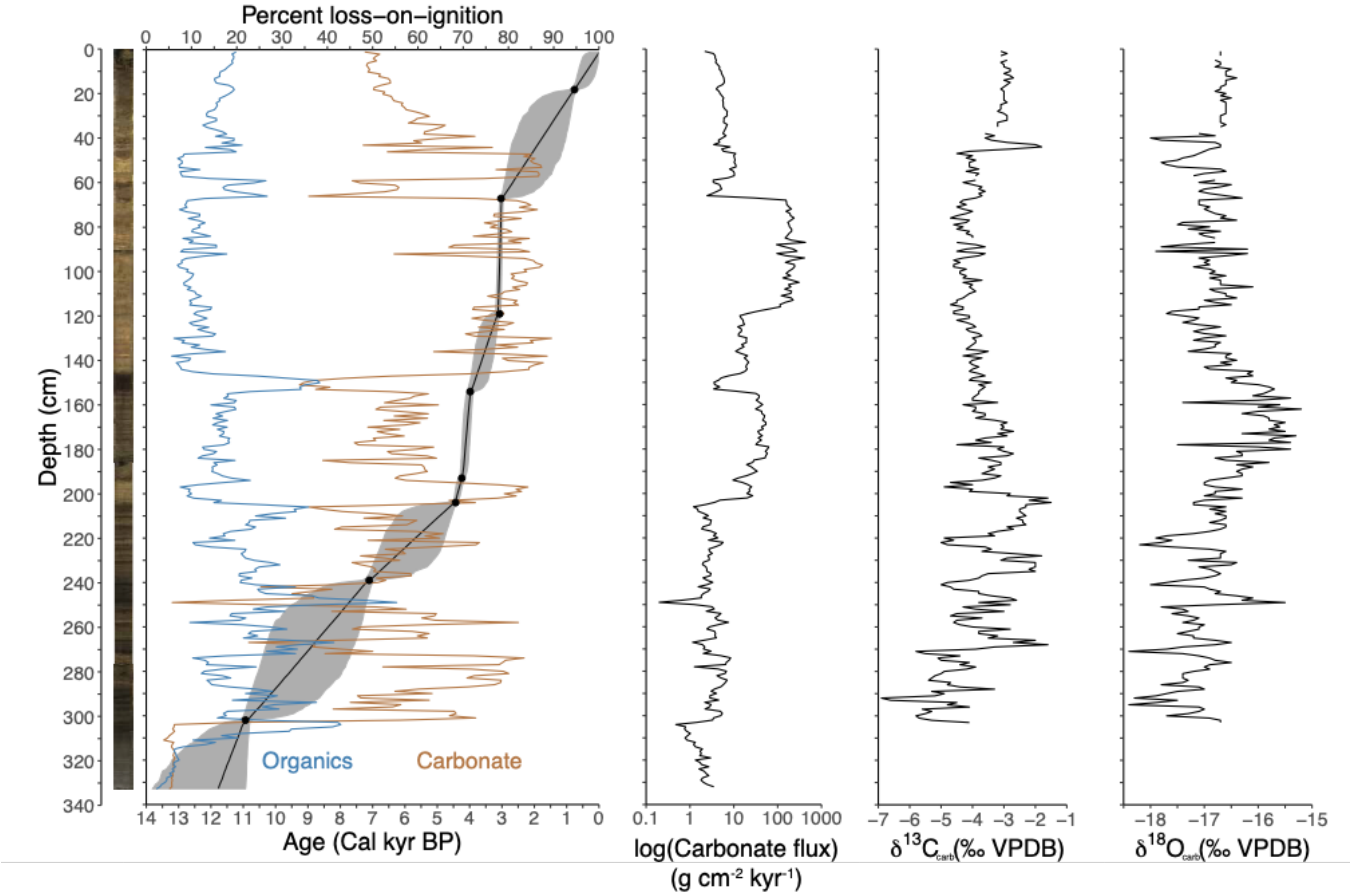

Figure 4. Percent organics, percent carbonate, carbonate flux, $\delta^{13}C_{carb}$, and $\delta^{18}O_{carb}$ are shown by depth alongside an image of the 333-cm-long sediment core from Highway 130 Lake. Radiocarbon ages (black dots) were used to create the age-depth model and gray uncertainty band (2 sigma).

4.3 Sedimentary oxygen and carbon isotopes

$\delta^{13}C_{carb}$ and $\delta^{18}O_{carb}$ in the upper 303 cm of sediment range from -6.9 to -1.5‰ and -18.4 to -15.2‰, respectively, and the mean isotope compositions become more positive over the record, but there is no significant trend (Fig. 4). Variance in $\delta^{13}C_{carb}$ and $\delta^{18}O_{carb}$ is highest before 4.4 ka (below 200-cm depth) and lowest since 1.5 ka (above 40-cm depth; Fig. 5). Isotope

289 excursions appear in both the slow and fast sedimentation intervals and when the carbonate flux
290 is both low and high (Fig. 4). $\delta^{18}O_{carb}$ peaks (2.9 standard deviations above the mean) from

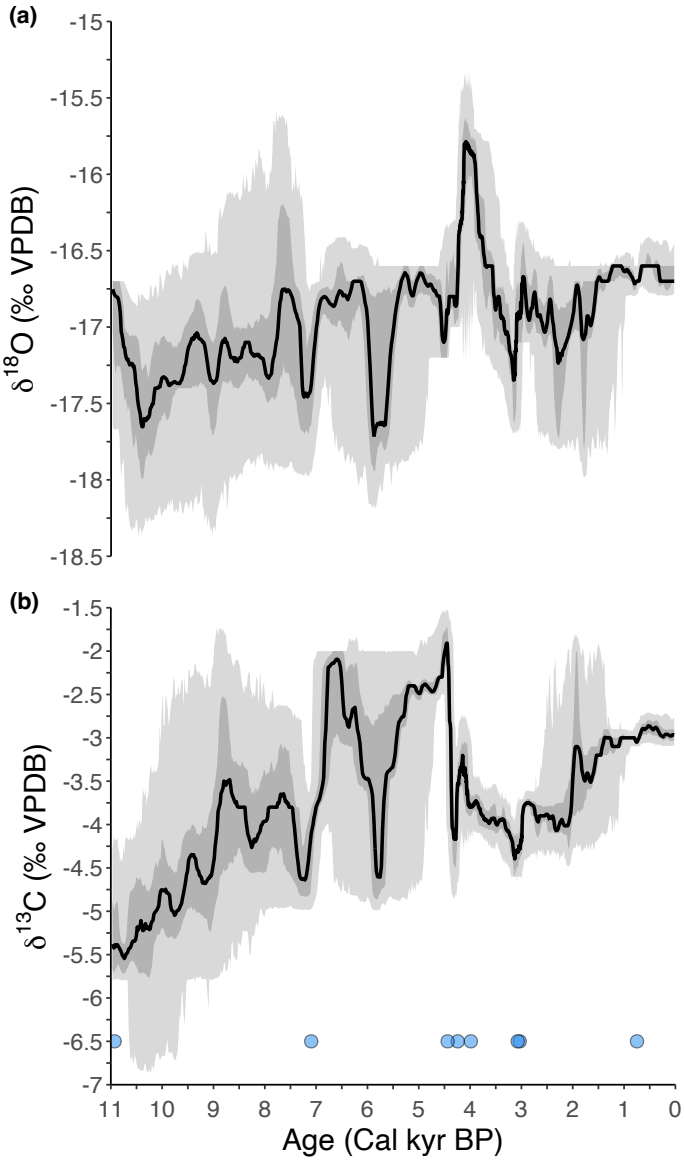

291

Figure 5. $\delta^{18}O_{carb}$ (a) and $\delta^{13}C_{carb}$ (b) from Highway 130 Lake. The black line represents the median estimate of the ensemble regression, and the dark and light gray bands show the 50% and 95% highest-probability density regions, respectively. The blue dots indicate the calibrated radiocarbon ages used for the age-depth model (refer to Table 2 for calibrated age uncertainties).

approximately 4.2–4 ka, where four calibrated radiocarbon ages constrain the timing and indicate a fast sedimentation rate (Fig. 5). The carbonate flux is high, but the carbonate content is low (~55%) during this interval relative to the mean (Fig. 4).

Compared to the records for Bison and Yellow Lakes in Colorado (Anderson, 2011, 2012; Fig. 1), $\delta^{18}O_{carb}$ values of HL are several per mil lower with higher variance for most of the Holocene (Fig. 6). This pattern changes in the late Holocene as carbonate in Bison Lake becomes isotopically lighter than before and approaches the oxygen isotope composition of HL, which maintains a relatively constant mean $\delta^{18}O_{carb}$ value. After approximately 1.5 ka, $\delta^{18}O_{carb}$ variability in HL drops to near the analytical uncertainty (± 0.2‰) while the other records show increased variably (Fig. 6). Despite an increase in summer lake-water $\delta^{18}O$ from -17.8 to -10.8‰ today (thick black line, Fig. 2), $\delta^{18}O_{carb}$ values at HL since 1.5 ka only reached a maximum of -16.4‰ and the core-top value is -16.7‰ (Fig. 5). Based on measured lake-water $\delta^{18}O$ and mean water temperatures during the biweekly intervals in which samples were collected from June through October, core-top $\delta^{18}O_{carb}$ at HL should range from -17.4 – -10.3‰ based on a standard $\delta^{18}O$-temperature model for estimating $\delta^{18}O_{carb}$ (Leng and Marshall, 2004); using the full range of lake-water temperatures measured through the annual cycle produces a range of -18.3 – -8.9‰.

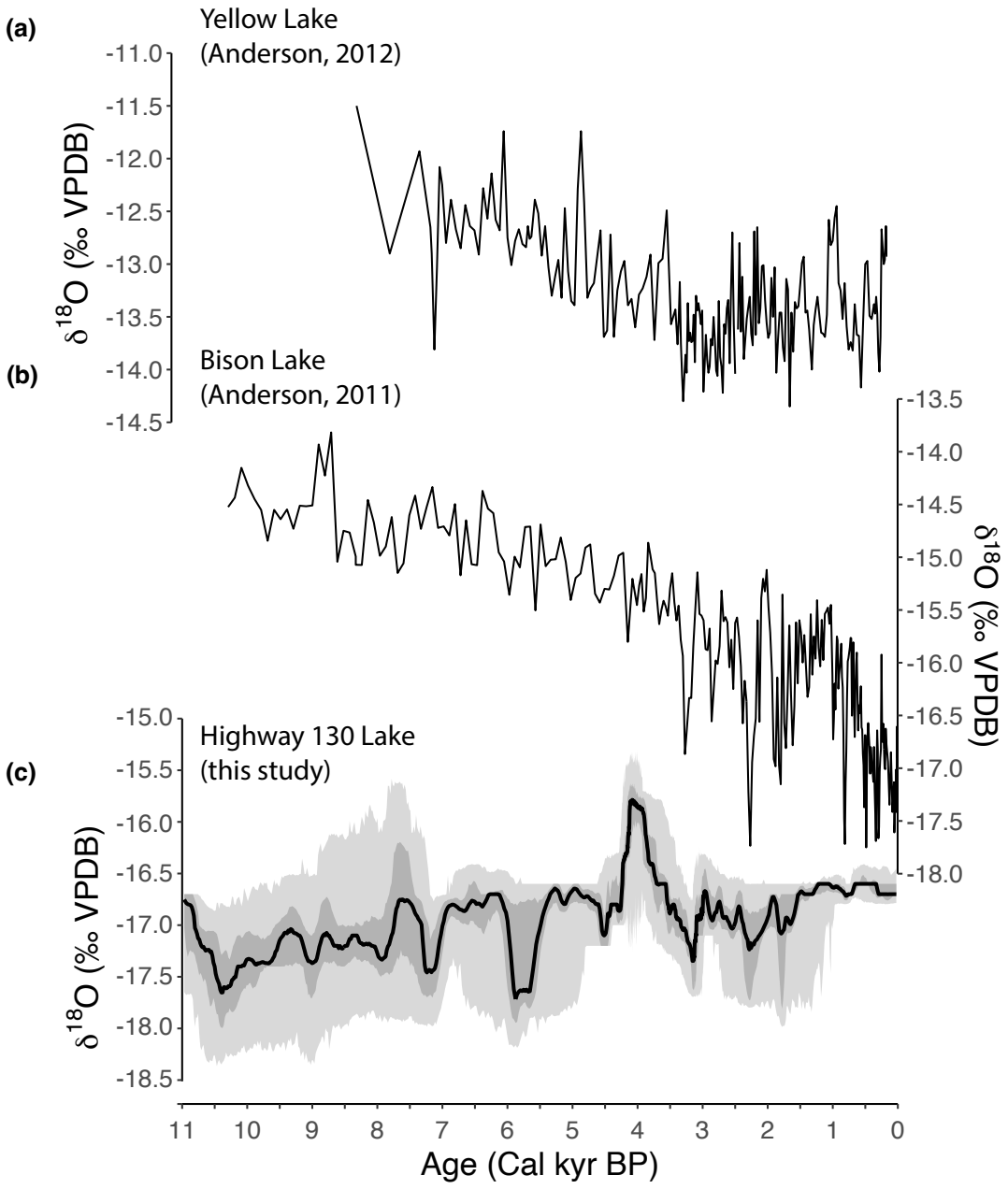

315

Figure 6. $\delta^{18}O_{carb}$ records from (a) Yellow Lake (Anderson, 2012), (b) Bison Lake (Anderson, 2011), and (c) Highway 130 Lake. In (c) the black line represents the median estimate of the ensemble regression, and the dark and light gray bands show the 50% and 95% highest-probability density regions, respectively.

316

5. **Discussion**

5.1 Evidence of the 4.2 ka drought in the southern Rocky Mountains

Peak $\delta^{18}O_{carb}$ in HL indicates an abrupt decline in effective moisture or at least a decline in the ratio of snowfall to rain in the Medicine Bow Mountains from approximately 4.2–4 ka (Fig. 5) when evidence from additional climate records shows that aridity affected the southern Rocky Mountains and portions of the Great Plains (Carter et al., 2013; Halfen & Johnson, 2013; Stokes & Gaylord, 1993). The isotope composition of mean annual precipitation potentially became heavier as snowfall declined relative to rain, causing HL's lake-water $\delta^{18}O$ and $\delta^{18}O_{carb}$ to increase. High evaporation could have also amplified these changes. The highest $\delta^{18}O_{carb}$ values at HL coincide with the pollen-inferred precipitation and temperature changes at 4.2 ka at Long Lake, which records two centuries of severe drought (Long Lake, Fig. 1; Carter et al., 2013). The excursion also aligns with the longstanding evidence of drought in the Great Plains and southern Rocky Mountains (dune fields, Fig. 1), where a rapid loss of grain-trapping vegetation likely triggered several centuries of increased aeolian transport documented across multiple dune fields (Booth et al., 2005; Forman et al., 2001; Halfen et al., 2010; Stokes & Gaylord, 1993).

Taken together, the records suggest that rapid drying at around 4.2 ka was an important climatic event in the Medicine Bow Mountains even if the drought is not a prominent feature in other paleoclimate studies from the mid-latitude Rocky Mountains (Anderson et al., 2008; Brunelle et al., 2013; Feiler et al., 1997; Johnson et al., 2013; Mensing et al., 2012; Minckley et al., 2012; Shuman et al., 2010; Thompson et al., 1993; Whitlock & Bartlein, 1993), including the nearby $\delta^{18}O_{carb}$ records from Bison and Yellow Lakes (Anderson, 2011, 2012). The spatial patterns of late-Holocene hydroclimate changes in North America may have been complex

compared to other regions, such as the European continent where late-Holocene climate variability appears more coherently in climate records (e.g., Deininger et al., 2017). For example, drought status can differ significantly east and west of the Continental Divide, which lies between HL and Bison Lakes. Still, the inconsistent evidence complicates interpretations of the 4.2 ka anomaly here and elsewhere (Bradley & Bakke, 2019).

Some paleohydrologic evidence indicates, however, that the event may have been extensive in the southern Rocky Mountains. Sedimentological changes in Little Molas, Emerald, and Upper Big Creek lakes, all high-elevation lakes in Colorado (Fig. 1, Table 1), show substantial hydrological transformation at around 4 ka matching the timing and scale of drought inferred from HL's record (Fig. 7; Shuman et al., 2009a, 2014, 2015). The sediment stratigraphies in these three lakes record low water levels that shifted shoreline sands to the locations of cores collected in 1–5-m water depth today and thus indicate reduced effective moisture at ca. 4.2–4 ka (orange shaded regions, Fig. 7). The median ages of sand layers, indicative of low water at these sites, overlap and fall within the age distribution of the elevated $\delta^{18}O_{carb}$ at HL and overlap with the ages of dune activity in southeast Wyoming (Halfen & Johnson, 2013; Stokes & Gaylord, 1993); the high-elevation lake locations and geophysical site surveys confirm that the shallow-water sands were not deposited by aeolian activity. Multiple radiocarbon ages also constrain the interval of high carbonate accumulation to approximately 4.4–3 ka, but the sedimentation rate in the interval is sensitive

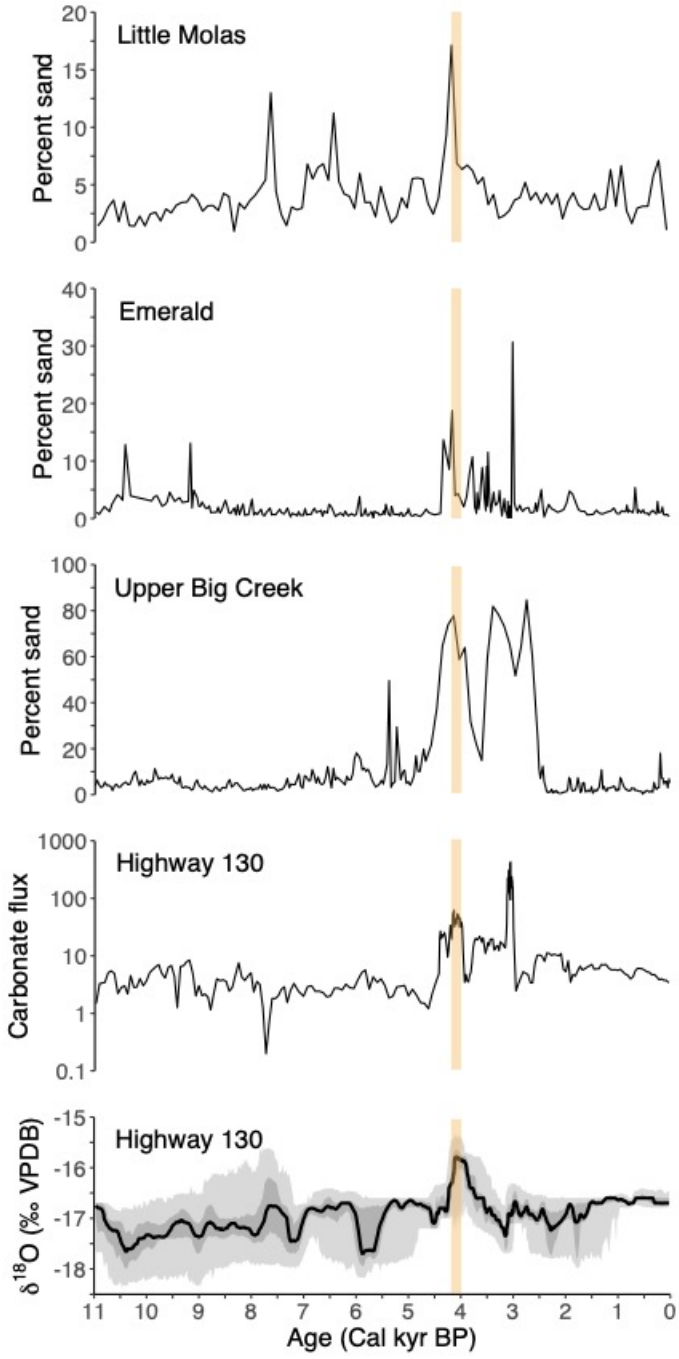

363

364

Figure 7. Spikes in the sand content of Little Molas, Emerald, and Upper Big Creek Lakes, located in high-elevation watersheds in Colorado (Fig. 1), align with the positive $\delta^{18}O_{carb}$ excursion at Highway 130 Lake and indicate low water from approximately 4.2–4 ka (orange shaded areas) resulting from low effective moisture (Shuman et al., 2009a, 2014, 2015).

to removal of one of the ages; if the age at ca. 3 ka is out of sequence, it may bias the peak rate of sediment and carbonate accumulation toward high values (but not the timing of the $\delta^{18}O_{carb}$ peak, Figures 4-7).

The rapid transition from deep-water muds to shallow-water sands as water levels dropped in the Colorado lakes at around 4.2 ka corresponds with changes in pollen assemblages in central Colorado (Jiménez-Moreno et al., 2019) and southeast Wyoming (Carter et al., 2013), as well as with other evidence for drought in North America (Fig. 1, Table 1; Booth et al., 2004). Similar sedimentological features found in lakes along the Atlantic margin from Maine to Pennsylvania date to around 4.2 ka, for example, where the drought appears as one of multiple events linked to circulation changes over the North Atlantic (Li et al., 2007; Marsicek et al., 2013; Newby et al., 2014; Nolan, 2020; Shuman et al., 2019; Shuman & Burrell, 2017). The sequences in the southern Rocky Mountains, however, include uniquely prominent sedimentological changes from ca. 4.2–4 ka, which align with the single large positive $\delta^{18}O_{carb}$ excursion at HL.

Given the growing evidence of drought within the southern Rocky Mountains at ca. 4.2 ka, a lack of $\delta^{18}O_{carb}$ records of the event in the region, or in North America entirely, is surprising (Anderson et al., 2016b; Konecky et al., 2020). However, individual sites respond to a varying mixture of local and regional factors. The stratigraphic evidence of lake-level change in the region is not entirely consistent either and may indicate interactions with different directions of hydroclimate change across seasons, elevations, and latitudes. Stratigraphic features in Hidden Lake, located in northern Colorado just south of Upper Big Creek Lake (Fig. 1) but several hundred meters lower in elevation, document a rapid increase in effective moisture at around 4 ka (Shuman et al., 2009)—the opposite response of the surrounding lakes at higher elevations

388 (Fig. 7). The wet phase was abrupt in onset and termination and lasted from around 4.4–3.7 ka,
389 based on multiple radiocarbon ages, and stands out amid an otherwise gradual trend towards
390 higher water levels since 6 ka (Shuman et al., 2009).
391 The low-elevation location of Hidden Lake may indicate an important role for increased
392 summer or fall rainfall when high-elevation lake levels declined in response to low winter
393 snowfall. Low winter snow can create favorable surface-energy conditions for strong summer
394 convective precipitation (Zhu et al. 2005). The combined effects could have favored the
395 unusually high $\delta^{18}O_{carb}$ at HL by positively shifting the isotope values of mean annual
396 precipitation and HL's water. Alternatively, the reversed hydrologic response of Hidden Lake
397 could indicate antiphased hydroclimate changes in the southern Rocky Mountains between high
398 and low elevations, which is consistent with modern responses to the El Niño-Southern
399 Oscillation (Preece et al., 2020). The active dune fields in east-central Wyoming, however, could
400 confound a simple interpretation of the elevational and seasonally antiphased hydrologic
401 changes, although their activity may depend on soil moisture derived from winter snow (Stokes
402 & Gaylord, 1993). Latitudinal hydroclimate variability could be an additional complicating
403 factor related to the dynamic boundary between the climates of the northern and southern Rocky
404 Mountains (Shinker, 2010; Wise, 2010). The comparison of the radiocarbon age uncertainties of
405 the 4.2 ka paleoshoreline sands at lake-level sites, including Emerald Lake in central Colorado
406 (Fig. 1 & 7), indicates a late-Holocene north-south moisture dipole extending across much of the
407 area described here (Shuman et al., 2014).
408 Given the potential prominence of the 4.2 ka drought at HL and other southern Rocky
409 Mountain records, it may have been uniquely severe in this region even if it had a complex
410 regional expression at broader spatial scales. The lake-level reconstructions from Colorado

411 contain evidence of other Holocene hydrologic changes (Fig. 7), but the records lack evidence
412 for multiple recurrent, multi-century hydroclimate changes recorded with the 4.2 ka event in
413 places like the Atlantic margin (Shuman et al., 2019). Elsewhere, aridity at 4.2 ka may represent
414 just one of several repeated drying events consistent with climate records and simulations from
415 around the world that show drought as a regular feature of late-Holocene climate variability (Arz
416 et al., 2006; Bradley & Bakke, 2019; Mayewski et al., 2004; Wanner et al., 2008; Wanner et al.,
417 2015; Yan & Liu, 2019). The mid-latitude Rocky Mountain records may suggest that the
418 midcontinent was insulated from some of the abrupt late-Holocene climate changes, possibly due
419 to its isolation from the ocean-atmosphere dynamics proposed to play key roles in Holocene
420 variability (Arz et al., 2006; Deininger et al., 2017; Jalali et al., 2019; Yan & Liu, 2019).
421
422 **5.2** ***Varying $\delta^{18}O_{carb}$ trends in the southern Rocky Mountains***
423 The marked sensitivity of lake-water $\delta^{18}O$ to hydroclimate changes may make lacustrine
424 carbonates ideal indicators of past droughts like the 4.2 ka event, as documented by $\delta^{18}O_{carb}$
425 records outside of North America (e.g., Bini et al., 2019; Dean et al., 2015) and by our record at
426 HL (Fig. 5), but site-specific hydrologic conditions could complicate the signals. They may
427 generate inconsistent trends among records over both short (seasonal) and long (millennial)
428 timescales (Gibson et al., 2016; Shapley et al., 2008; Steinman & Abbott, 2013; Tyler et al.,
429 2007). Indeed, we observe such inconsistency in the southern Rocky Mountains (Fig. 6).
430 The hydrologic controls, such as groundwater fluxes and basin morphology, can vary
431 based on a lake's geohydrological setting (Anderson et al., 2016; Dean et al., 2015). Modern
432 lake-water hydrogen and oxygen isotope measurements reveal stronger fractionation by
433 evaporation in HL (thick black line, Fig. 2) compared to Bison and Yellow Lakes (purple and

yellow lines, Fig. 2; Anderson, 2012), which exhibit a narrower range in modern water isotope compositions and smaller deviation from the global meteoric water line. The differences in hydrologic setting at each lake that produce this pattern are not assumed to override changes in lake-water $\delta^{18}O$ due to climate changes, such as drought. However, the isotopically light carbonate at HL (Fig. 6) is antithetical to the expectation based on evaporatively enriched summer waters (Fig. 2) and suggests that the site may have been sensitive to seasonal dynamics not recorded by Bison or Yellow Lakes. The pattern differs from the interpretation that the Bison Lake $\delta^{18}O_{carb}$ was not strongly influenced by evaporation because it was isotopically lighter than other sites like Yellow Lake (Anderson, 2011, 2012). Given the modern water isotope values, we had anticipated that $\delta^{18}O_{carb}$ from HL would be isotopically heavy compared to Bison and Yellow Lakes, but track similar trends (Anderson, 2012). However, HL lacks the prominent $\delta^{18}O_{carb}$ trend observed at these other sites (Fig. 6).

Differences in the timing of carbonate formation could explain the variability among the records and their sensitivity to the 4.2 ka event. Because rain is isotopically heavier than snow, decreasing snowpack in the watershed should positively shift the isotope composition of HL's water and carbonates. A lower ratio of precipitation to evaporation could also cause a positive shift if carbonates form in evaporated summer waters; however, if the precipitation of carbonates occurs during winter or spring, then $\delta^{18}O_{carb}$ would track the relative contributions of snowfall and rain to its water balance without modification by summer evaporation. Previous studies have shown that the deposition of endogenic carbonate occurs predominantly in the warm summer months when photosynthesis optimizes carbonate production by modifying dissolved CO_2 concentrations and pH (Leng & Marshall, 2004), but the isotopically light carbonate at HL may contradict this expectation. The observed core-top $\delta^{18}O_{carb}$ value is lower than the calculated

457 fractionation of calcite formation in summer waters, which indicates that HL may not integrate
458 the range of summer lake-water $\delta^{18}O$ today as is assumed for Bison and Yellow Lakes (and
459 carbonate lakes in general).

460 We observe the same pattern in HL's sediment record. $\delta^{18}O_{carb}$ values were below the
461 mean at 6 ka (Fig. 5) when simulated estimates of evaporation rates in the Medicine Bow
462 Mountains were up to 30% higher than today (Morrill et al., 2019). The enhanced evaporation
463 may explain the more positive mid-Holocene $\delta^{18}O_{carb}$ at Bison and Yellow lakes relative to today
464 (Fig. 6), but if so, such enhanced summer evaporation did not affect $\delta^{18}O_{carb}$ at HL. Because the
465 early springtime deposition of carbonate could capture the isotopic signature of the lake water
466 early in the year, HL may be a better indicator of the snow-to-rain ratio represented by the
467 groundwater inflow into the lake than the seasonal isotopic enrichment of the lake waters by
468 evaporation later in the summer.

469 The year-round measurements of specific conductance show that conditions favorable for
470 carbonate precipitation may indeed be highest during late winter and spring. In 2017, specific
471 conductance of the water below the surface ice rose from 700 μS/cm in early February to 1,115
472 μS/cm by early April, and it remained above 1,000 μS/cm throughout April (Fig. 3). These high
473 values would favor carbonate precipitation, whereas the summertime waters are more dilute.
474 Specific conductance of HL and other lakes within the watershed during the summer typically
475 does not exceed 300 μS/cm. Melting of lake ice and snowpack rapidly lowers the specific
476 conductance by early May and it remains between 250–300 μS/cm for the remaining ice-free
477 months. The conductance likely remains lower than in winter despite evaporative enrichment of
478 the oxygen isotopes because of groundwater discharge into the lake (Rautio & Korkka-Niemi,
479 2011), which geophysical surveys, water temperatures, and stable summer water levels at HL

480 support (Liefert et al., 2018). If so, ions exsolved from overlying ice raise the conductance of the
481 lake water and pore water within the bottom sediments beyond the concentration in groundwater
482 in winter (Adams & Lasenby, 1985), and create favorable conditions for the rapid deposition of
483 endogenic carbonate in early spring when the isotopic signal would not reflect evaporation or
484 isotopically heavy summer rainfall (open circles, Fig. 2). Spring carbonate formation could also
485 yield a different temperature-dependent effect on the $\delta^{18}O_{carb}$ in HL compared to the other lakes,
486 but the cold spring waters at HL should favor an increase, not decrease, in $\delta^{18}O_{carb.}$ Indeed, all of
487 the readily expected process that could complicate a carbonate isotopic record should drive the
488 $\delta^{18}O_{carb}$ in the positive (not negative) direction and underscore the significance of the difference
489 between HL and the other lakes.
490 As an alternative explanation, the $\delta^{18}O_{carb}$ values could reflect changes in total
491 precipitation rather than seasonality effects because the inflow of Ca-bearing groundwater
492 (which should rise with precipitation) can increase carbonate production and lower $\delta^{18}O_{carb}$
493 values in alkaline lakes in both ice-free and ice-covered conditions (Shapley et al., 2005), but the
494 weak covariance of weight percent carbonate and $\delta^{18}O_{carb}$ suggest that rates of groundwater
495 inflow did not strongly influence $\delta^{18}O_{carb}$ (Fig. S1a). A weak covariance of $\delta^{13}C_{carb}$ and $\delta^{18}O_{carb}$
496 indicates short lake-water residence times throughout the lake's history (Fig. S1b; Drummond et
497 al., 1995; Talbot & Kelts, 1990), which could be consistent with rapid flowthrough that reduced
498 evaporative enrichment; removing values from 4.2-4 ka only marginally improves the
499 correlation.
500 A strong negative correlation of weight percent organics and carbonate ($R^2 = –0.79$)
501 suggests that carbonate abundance depends primarily on biological productivity that promoted
502 carbonate dissolution by releasing CO_2 and lowering pH (Fig S1c; Dean, 1999). Carbonate

503 content from 4.2–4 ka was below the mean despite low organic content (red dots, Fig. S1c) and a
504 high flux of carbonate (Fig. 4), which may represent a shift in HL's water levels and chemistry
505 that favored both acidic conditions and isotopically heavy carbonate (red dots, Fig. S1). Down-
506 core shifts in $\delta^{18}O_{carb}$ produced by seasonal changes in the timing and rate of carbonate formation
507 have been proposed as potential sources of variability within individual records (Fronval et al.,
508 1995; Lamb et al., 2007; Steinman et al., 2012; Steinman & Abbott, 2013; Tyler et al., 2007) and
509 could play a role in the record at HL, but such differences could also generate the variability in
510 the long-term trends observed among records from the southern Rocky Mountains and elsewhere
511 (Bini et al., 2019; Konecky et al., 2020; Roberts et al., 2008).

512 Many non-climatic factors influence $\delta^{18}O_{carb}$, including carbonate phase and disequilibrium
513 effects, seasonality of precipitation, groundwater fluxes, the isotope compositions of precipitation
514 and groundwater, and local geology. However, such factors are unlikely sources of variability
515 among the regional $\delta^{18}O_{carb}$ records. Down-core carbonate phase changes are unlikely as only
516 calcite was present in the cores from HL, Bison Lake, and Yellow Lake. We also find no
517 evidence in the sediment core or modern setting at HL to indicate that anthropogenic influence or
518 biologically mediated precipitation of calcite substantially altered $\delta^{18}O_{carb}$ (e.g., carbonate
519 ostracod tests formed in disequilibrium with lake water). Disequilibrium effects associated with
520 biogenic carbonates generally increase $\delta^{18}O_{carb}$ (Holmes & Chivas, 2002; Leng & Marshall,
521 2004), which would be difficult to reconcile with the surprisingly negative mean and core-top
522 $\delta^{18}O_{carb}$ values at HL based on expectations from the strong enrichment of heavy isotopes by
523 evaporation today and predicted core-top $\delta^{18}O_{carb}$ values.

524 The seasonal balance of precipitation today is broadly similar among the sites (inset plot,
525 Fig. 2) and the calculated annual precipitation-$\delta^{18}O$ value is approximately 1‰ lower at HL than

526 at Bison and Yellow Lakes (http://waterisotopesDB.org). Annual temperature ranges are also
527 similar for the watersheds, making it unlikely that temperature dependence of fractionation could
528 explain the range in $\delta^{18}O_{carb}$ values recorded across the three records unless the different water
529 depths and groundwater influences altered the seasonal temperature progression among lakes.
530 The difference in temperature would need to be large (~12 °C) to explain the offset in $\delta^{18}O_{carb}$
531 between HL and Bison Lake (and larger for the offset between HL and Yellow Lake), which is
532 unrealistic given the sites' comparable locations and elevations and the relatively small
533 temperature changes at mid-latitudes since 11 ka (Marsicek et al., 2018). The range in $\delta^{18}O_{carb}$
534 calculated from the annual range in modern lake-water $\delta^{18}O$ at the lakes does match the observed
535 offsets in the $\delta^{18}O_{carb}$ records of HL, Bison, and Yellow Lakes. The timing of carbonate
536 formation thus remains a plausible mechanism for producing the differences. Installing sediment
537 traps during the ice-free season could test the timing of carbonate production.
538
539 ## 6. **Conclusions**
540 $\delta^{18}O_{carb}$ from HL indicates an abrupt hydroclimate change in the southern Rocky
541 Mountains from approximately 4.2–4 ka that reduced effective moisture or caused less snow to
542 fall than today at high elevations in southern Wyoming. Other $\delta^{18}O_{carb}$ records from the region
543 do not document the drought (Fig. 6; Anderson, 2012), but the event's timing overlaps with
544 evidence of multi-century drought from pollen, lake stratigraphies, and dunes in the southern
545 Rocky Mountains (Carter et al., 2013; Halfen & Johnson, 2013; Shuman et al., 2009a, 2014,
546 2015; Stokes & Gaylord, 1993), the western Great Plains (Booth et al., 2005; Dean, 1997; Halfen
547 & Johnson, 2013; Mason et al., 1997; Stokes & Gaylord, 1993), and elsewhere around the world
548 (Nakamura et al., 2016; Di Rita & Magri, 2019; Scuderi et al., 2019; Xiao et al., 2018).

549 The timing and magnitude of hydroclimate change in our record agrees with the
550 perspective of a widespread megadrought at around 4.2 ka (Weiss, 2016), but inconsistencies
551 among climate records suggests that (1) site-specific factors can prevent identification of the
552 patterns of abrupt hydroclimate changes, particularly in $\delta^{18}O_{carb}$ records; (2) the hydrologic
553 response in North America and likely elsewhere around the world was spatially complex; and (3)
554 the abrupt hydroclimate changes in the North American midcontinent were more pronounced
555 against background Holocene variability than in many regions such as the Atlantic margin.
556 Consequently, a prolonged 'megadrought' at 4.2 ka was likely a significant feature of the
557 hydroclimate history in the mid-latitude Rocky Mountains even if that is not true globally.
558
559 **Data availability**
560 Data related to this paper are available through the National Centers for Environmental
561 Information on the National Oceanic and Atmospheric Administration website:
562 https://www.ncdc.noaa.gov/paleo/study/34993. The analyses were performed in R.
563
564 **Author contributions**
565 D. Liefert and B. Shuman contributed to the design and implementation of the research, to the
566 analysis of the results, and to the writing of the manuscript.
567
568 **Competing Interests**
569 The authors declare that they have no conflict of interest.
570
571 **Acknowledgments**

572 This project was funded by the National Geographic Society (CP-064ER-17), U.S. National
573 Science Foundation P2C2 (EAR-1903729), the Wyoming Center for Environmental Hydrology
574 and Geophysics via support from the U.S. NSF EPSCoR program (EPS-1208909), and the
575 Department of Geology and Geophysics at the University of Wyoming. We thank Andrew
576 Parsekian and Kevin Befus for field assistance and Andrew Flaim for assisting in sample
577 preparation.

578

579 **References**

580 Adams, W. P., & Lasenby, D. C. (1985). The Roles of Snow, Lake Ice and Lake Water in the Distribution of Major
581 Ions in the Ice Cover of a Lake. *Annals of Glaciology*, *7*(February 1979), 202–207.
582 https://doi.org/10.3189/s0260305500006170

583 Alley, R. B., Mayewski, P. A., Sowers, T., Stuiver, M., Taylor, K. C., & Clark, P. U. (1997). Holocene climatic
584 instability: A prominent, widespread event 8200 yr ago. *Geology*, *25*(6), 483–486.
585 https://doi.org/10.1130/0091-7613(1997)025<0483:HCIAPW>2.3.CO;2

586 Anderson, L. (2011). Holocene record of precipitation seasonality from lake calcite δ18O in the central Rocky
587 Mountains, United States. *Geology*, *39*(3), 211–214. https://doi.org/10.1130/G31575.1

588 Anderson, L. (2012). Rocky Mountain hydroclimate: Holocene variability and the role of insolation, ENSO, and the
589 North American Monsoon. *Global and Planetary Change*, *92–93*, 198–208.
590 https://doi.org/10.1016/j.gloplacha.2012.05.012

591 Anderson, L., Berkelhammer, M., Barron, J. A., Steinman, B. A., Finney, B. P., & Abbott, M. B. (2016a). Lake
592 oxygen isotopes as recorders of North American Rocky Mountain hydroclimate: Holocene patterns and
593 variability at multi-decadal to millennial time scales. *Global and Planetary Change*, *137*, 131–148.
594 https://doi.org/10.1016/j.gloplacha.2015.12.021

595 Anderson, L., Berkelhammer, M., Barron, J. A., Steinman, B. A., Finney, B. P., & Abbott, M. B. (2016b). Lake
596 oxygen isotopes as recorders of North American Rocky Mountain hydroclimate: Holocene patterns and
597 variability at multi-decadal to millennial time scales. *Global and Planetary Change*, *137*, 131–148.
598 https://doi.org/10.1016/j.gloplacha.2015.12.021

599 Anderson, R. S., Allen, C. D., Toney, J. L., Jass, R. B., & Bair, A. N. (2008). Holocene vegetation and fire regimes
600 in subalpine and mixed conifer forests, southern Rocky Mountains, USA. *International Journal of Wildland*
601 *Fire*, *17*(1), 96. https://doi.org/10.1071/WF07028
602 Arz, H. W., Lamy, F., & Pätzold, J. (2006). A pronounced dry event recorded around 4.2 ka in brine sediments from
603 the northern Red Sea. *Quaternary Research*, *66*(3), 432–441. https://doi.org/10.1016/j.yqres.2006.05.006
604 Ault, T. R., George, S. S., Smerdon, J. E., Coats, S., Mankin, J. S., Carrillo, C. M., et al. (2018). A robust null
605 hypothesis for the potential causes of megadrought in Western North America. *Journal of Climate*, *31*(1), 3–
606 24. https://doi.org/10.1175/JCLI-D-17-0154.1
607 Bello, R., & Smith, J. D. (1990). The Effect of Weather Variability on the Energy Balance of a Lake in the Hudson
608 Bay Lowlands , Canada. *INSTAAR, University of Colorado*, *22*(1), 98–107.
609 Bini, M., Zanchetta, G., Perşoiu, A., Cartier, R., Català, A., Cacho, I., et al. (2019). The 4.2 ka BP Event in the
610 Mediterranean region: An overview. *Climate of the Past*, *15*(2), 555–577. https://doi.org/10.5194/cp-15-555-
611 2019
612 Booth, R. K., Jackson, S. T., Forman, S. L., Kutzbach, J. E., Bettis, E. A., Kreig, J., & Wright, D. K. (2005). A
613 severe centennial-scale drought in mid-continental North America 4200 years ago and apparent global
614 linkages. *Holocene*, *15*(3), 321–328. https://doi.org/10.1191/0959683605hl825ft
615 Bradley, R. S., & Bakke, J. (2019). Is there evidence for a 4.2 ka BP event in the northern North Atlantic region?
616 *Climate of the Past*, *15*(5), 1665–1676. https://doi.org/10.5194/cp-15-1665-2019
617 Brunelle, A., Minckley, T. A., Lips, E., & Burnett, P. (2013). A record of Lateglacial/Holocene environmental
618 change from a high-elevation site in the Intermountain West, USA. *Journal of Quaternary Science*, *28*(1),
619 103–112. https://doi.org/10.1002/jqs.2600
620 Carter, V. A., Brunelle, A., Minckley, T. A., Dennison, P. E., & Power, M. J. (2013). Regionalization of fire regimes
621 in the Central Rocky Mountains, USA. *Quaternary Research (United States)*, *80*(3), 406–416.
622 https://doi.org/10.1016/j.yqres.2013.07.009
623 Carter, V. A., Shinker, J. J., & Preece, J. (2018). Drought and vegetation change in the central Rocky Mountains and
624 western Great Plains: Potential climatic mechanisms associated with megadrought conditions at 4200 cal yr
625 BP. *Climate of the Past*, *14*(8), 1195–1212. https://doi.org/10.5194/cp-14-1195-2018
626 Clark, P. U., Webb, R. S., & Keigwin, L. D. (1999). *Mechanisms of global climate change at millennial time scales*.

Washington, DC: American Geophysical Union.

Dean, J. R., Jones, M. D., Leng, M. J., Noble, S. R., Metcalfe, S. E., Sloane, H. J., et al. (2015). Eastern Mediterranean hydroclimate over the late glacial and Holocene, reconstructed from the sediments of Nar lake, central Turkey, using stable isotopes and carbonate mineralogy. *Quaternary Science Reviews*, *124*, 162–174. https://doi.org/10.1016/j.quascirev.2015.07.023

Dean, W. E. (1997). Rates, timing, and cyclicity of Holocene eolian activity in north-central United States: Evidence from varved lake sediments. *Geology*, *25*(4), 331–334. https://doi.org/10.1130/0091-7613(1997)025<0331:RTACOH>2.3.CO;2

Dean, W. E. (1999). The carbon cycle and biogeochemical dynamics in lake sediments. *Journal of Paleolimnology*, *21*(4), 375–393. https://doi.org/10.1023/A:1008066118210

Deininger, M., McDermott, F., Mudelsee, M., Werner, M., Frank, N., & Mangini, A. (2017). Coherency of late Holocene European speleothem δ18O records linked to North Atlantic Ocean circulation. *Climate Dynamics*, *49*(1–2), 595–618. https://doi.org/10.1007/s00382-016-3360-8

Denniston, R. F., Gonzalez, L. A., Baker, R. G., Asmerom, Y., Reagan, M. K., Edwards, R. L., & Alexander, E. C. (1992). Speleothem evidence for Holocene fluctuations of the prairie-forest c cot one , *6*, 671–676.

Drummond, C. N., Patterson, W. P., & Walker, J. C. G. (1995). Climatic forcing of carbon-oxygen isotopic covariance in temperate-region marl lakes. *Geology*, *23*(11), 1031. https://doi.org/10.1130/0091-7613(1995)023<1031:cfocoi>2.3.co;2

Feiler, E. J., Scott, R., & Koehler, A. (2017). Late Quaternary Paleoenvironments of the White River Plateau , Colorado , U . S . A . Author (s): Eric J . Feiler , R . Scott Anderson and Peter A . Koehler Published by : INSTAAR , University of Colorado Stable URL : http://www.jstor.org/stable/1551836, *29*(1), 53–62.

Forman, S. L., Oglesby, R., & Webb, R. S. (2001). Temporal and spatial patterns of Holocene dune activity on the Great Plains of North America: Megadroughts and climate links. *Global and Planetary Change*, *29*(1–2), 1–29. https://doi.org/10.1016/S0921-8181(00)00092-8

Fronval, T., Jensen, N. B., & Buchardt, B. (1995). Oxygen isotope disequilibrium precipitation of calcite in Lake Arreso, Denmark. *Geology*, *23*(5), 463–466. https://doi.org/10.1130/0091-7613(1995)023<0463:OIDPOC>2.3.CO;2

Gibson, J. J., Birks, S. J., Yi, Y., Moncur, M. C., & McEachern, P. M. (2016). Stable isotope mass balance of fifty

lakes in central Alberta: Assessing the role of water balance parameters in determining trophic status and lake level. *Journal of Hydrology: Regional Studies*, *6*, 13–25. https://doi.org/10.1016/j.ejrh.2016.01.034

Von Grafenstein, U., Erlenkeuser, H., Müller, J., Jouzel, J., & Johnsen, S. (1998). The cold event 8200 years ago documented in oxygen isotope records of precipitation in Europe and Greenland. *Climate Dynamics*, *14*(2), 73–81. https://doi.org/10.1007/s003820050210

Halfen, A. F., & Johnson, W. C. (2013). A review of Great Plains dune field chronologies. *Aeolian Research*, *10*, 135–160. https://doi.org/10.1016/j.aeolia.2013.03.001

Halfen, A. F., Fredlund, G. G., & Mahan, S. A. (2010). Holocene stratigraphy and chronology of the Casper Dune Field, Casper, Wyoming, USA. *Holocene*, *20*(5), 773–783. https://doi.org/10.1177/0959683610362812

Henderson, A. K., & Shuman, B. N. (2009). Hydrogen and oxygen isotopic compositions of lake water in the western United States. *Geological Society of America Bulletin*, *121*(7–8), 1179–1189. https://doi.org/10.1130/B26441.1

Holmes, J. A., & Chivas, A. R. (2002). Ostracod shell chemistry—overview. *Geophysical Union Geophysical Monograph Series*, *131*, 185–204.

Houston, R. S., & Karlstrom, K. E. (1992). Geologic map of Precambrian metasedimentary rocks of the Medicine Bow Mountains, Albany and Carbon counties, Wyoming. *U.S. Geological Survey Miscellaneous Investigations Map*, *I-2280. Sc*.

Huang, C. C., Pang, J., Zha, X., Su, H., & Jia, Y. (2011). Extraordinary floods related to the climatic event at 4200 a BP on the Qishuihe River, middle reaches of the Yellow River, China. *Quaternary Science Reviews*, *30*(3–4), 460–468. https://doi.org/10.1016/j.quascirev.2010.12.007

Jalali, B., Sicre, M. A., Azuara, J., Pellichero, V., & Combourieu-Nebout, N. (2019). Influence of the North Atlantic subpolar gyre circulation on the 4.2 ka BP event. *Climate of the Past*, *15*(2), 701–711. https://doi.org/10.5194/cp-15-701-2019

Jiménez-Moreno, G., Anderson, R. S., Shuman, B. N., & Yackulic, E. (2019). Forest and lake dynamics in response to temperature, North American monsoon and ENSO variability during the Holocene in Colorado (USA). *Quaternary Science Reviews*, *211*, 59–72. https://doi.org/10.1016/j.quascirev.2019.03.013

Johnson, B. G., Jiménez-Moreno, G., Eppes, M. C., Diemer, J. A., & Stone, J. R. (2013). A multiproxy record of postglacial climate variability from a shallowing, 12-m deep sub-alpine bog in the southeastern San Juan

Mountains of Colorado, USA. *The Holocene*, *23*(7), 1028–1038. https://doi.org/10.1177/0959683613479682

Kahle, D., & Wickham, H. (2013). ggmap: Spatial Visualization with ggplot2. *The R Journal*, *5*(1), 144–161.

Konecky, B. L., Mckay, N. P., Sidorova, O. V. C., Comas-bru, L., Dassié, P., Delong, K. L., et al. (2020). The Iso2k Database: A global compilation of paleo-δ18O and δ^2H records to aid understanding of Common Era climate. *Earth Syst. Sci. Data Discuss.*, (In review). Retrieved from https://doi.org/10.5194/essd-2020-5

Lamb, H. F., Leng, M. J., Telford, R. J., Ayenew, T., & Umer, M. (2007). Oxygen and carbon isotope composition of authigenic carbonate from an Ethiopian lake: A climate record of the last 2000 years. *Holocene*, *17*(4), 517–526. https://doi.org/10.1177/0959683607076452

Leng, M. J., & Marshall, J. D. (2004). Palaeoclimate interpretation of stable isotope data from lake sediment archives. *Quaternary Science Reviews*, *23*(7–8), 811–831. https://doi.org/10.1016/j.quascirev.2003.06.012

Li, Y. X., Yu, Z., & Kodama, K. P. (2007). Sensitive moisture response to Holocene millennial-scale climate variations in the Mid-Atlantic region, USA. *Holocene*, *17*(1), 3–8. https://doi.org/10.1177/0959683606069386

Liefert, D. T., Shuman, B. N., Parsekian, A. D., & Mercer, J. J. (2018). Why Are Some Rocky Mountain Lakes Ephemeral? *Water Resources Research*, *54*(8), 5245–5263. https://doi.org/10.1029/2017WR022261

Marsicek, J., Shuman, B. N., Bartlein, P. J., Shafer, S. L., & Brewer, S. (2018). Reconciling divergent trends and millennial variations in Holocene temperatures. *Nature*, *554*(7690), 92–96. https://doi.org/10.1038/nature25464

Marsicek, J. P., Shuman, B., Brewer, S., Foster, D. R., & Oswald, W. W. (2013). Moisture and temperature changes associated with the mid-Holocene Tsuga decline in the northeastern United States. *Quaternary Science Reviews*, *80*, 129–142. https://doi.org/10.1016/j.quascirev.2013.09.001

Mason, J. P., Swinehart, J. B., & Loope, D. B. (1997). Holocene history of lacustrine and marsh sediments in a dune-blocked drainage, Southwestern Nebraska Sand Hills, U.S.A. *Journal of Paleolimnology*, *17*(1), 67–83. https://doi.org/10.1023/A:1007917110965

Mayewski, P. A., Rohling, E. E., Stager, J. C., Karlén, W., Maasch, K. A., Meeker, L. D., et al. (2004). Holocene climate variability. *Quaternary Research*, *62*(3), 243–255. https://doi.org/10.1016/j.yqres.2004.07.001

McKay, N. P., Emile-Geay, J., and Khider, D.: geoChronR – an R package to model, analyze, and visualize age-uncertain data, Geochronology, 3, 149–169, https://doi.org/10.5194/gchron-3-149-2021, 2021.

711 Mensing, S., Korfmacher, J., Minckley, T., & Musselman, R. (2012). A 15,000 year record of vegetation and
712 climate change from a treeline lake in the Rocky Mountains, Wyoming, USA. *The Holocene*, *22*(7), 739–748.
713 https://doi.org/10.1177/0959683611430339
714 Minckley, T. A., Shriver, R. K., & Shuman, B. (2012). Resilience and regime change in a southern Rocky Mountain
715 ecosystem during the past 17000 years TL - 82. *Ecological Monographs*, *82 VN-r*(1), 49–68.
716 https://doi.org/10.1890/11-0283.1
717 Mock, C. . (1996). Climate controls and spatial variations of precipitation in the western United States. *Journal of*
718 *Climate*, *9*, 1111–1125.
719 Morrill, C., Meador, E., Livneh, B., Liefert, D. T., & Shuman, B. N. (2019). Quantitative model-data comparison of
720 mid-Holocene lake-level change in the central Rocky Mountains. *Climate Dynamics*, *0*(0), 0.
721 https://doi.org/10.1007/s00382-019-04633-3
722 Musselman, R. C., Connell, B. H., Conrad, M. A., Dufford, R. G., Fox, D. G., Haines, J. D., et al. (1992). The
723 Glacier Lakes Ecosystem Experiments Site.
724 Nakamura, A., Yokoyama, Y., Maemoku, H., Yagi, H., Okamura, M., Matsuoka, H., et al. (2016). Weak monsoon
725 event at 4.2 ka recorded in sediment from Lake Rara, Himalayas. *Quaternary International*, *397*, 349–359.
726 https://doi.org/10.1016/j.quaint.2015.05.053
727 Newby, P. E., Shuman, B. N., Donnelly, J. P., Karnauskas, K. B., & Marsicek, J. (2014). Centennial-to-millennial
728 hydrologic trends and variability along the North Atlantic Coast, USA, during the Holocene. *Geophysical*
729 *Research Letters*, *41*(12), 4300–4307. https://doi.org/10.1002/2014GL060183
730 Nolan, C. (2020). *Using Co-Located Lake and Bog Records to Improve Inferences on Late Quaternary Climate and*
731 *Ecology*.
732 Parnell, A. C., Haslett, J., Allen, J. R. M., Buck, C. E., & Huntley, B. (2008). A flexible approach to assessing
733 synchroneity of past events using Bayesian reconstructions of sedimentation history. *Quaternary Science*
734 *Reviews*, *27*(19–20), 1872–1885. https://doi.org/10.1016/j.quascirev.2008.07.009
735 Preece, J. R., Shinker, J. J., Riebe, C. S., & Minckley, T. A. (2020). Elevation-dependent precipitation response to El
736 Niño-Southern oscillation revealed in headwater basins of the US central Rocky Mountains. *International*
737 *Journal of Climatology*, (November 2019), 1–12. https://doi.org/10.1002/joc.6790
738 Railsback, L. B., Liang, F., Brook, G. A., Voarintsoa, N. R. G., Sletten, H. R., Marais, E., et al. (2018). The timing,

two-pulsed nature, and variable climatic expression of the 4.2 ka event: A review and new high-resolution stalagmite data from Namibia. *Quaternary Science Reviews*, *186*, 78–90. https://doi.org/10.1016/j.quascirev.2018.02.015

Ran, M., & Chen, L. (2019). The 4.2 ka BP climatic event and its cultural responses. *Quaternary International*, (April), 0–1. https://doi.org/10.1016/j.quaint.2019.05.030

Rautio, A., & Korkka-Niemi, K. (2011). Characterization of groundwater-lake water interactions at Pyhäjärvi, a lake in SW Finland. *Boreal Environment Research*, *16*(5), 363–380.

Renssen, H., Goosse, H., & Muscheler, R. (2006). Coupled climate model simulation of Holocene cooling events: oceanic feedback amplifies solar forcing, 79–90.

Di Rita, F., & Magri, D. (2019). The 4.2 ka event in the vegetation record of the central Mediterranean. *Climate of the Past*, *15*(1), 237–251. https://doi.org/10.5194/cp-15-237-2019

Roberts, N., Jones, M. D., Benkaddour, A., Eastwood, W. J., Filippi, M. L., Frogley, M. R., et al. (2008). Stable isotope records of Late Quaternary climate and hydrology from Mediterranean lakes: the ISOMED synthesis. *Quaternary Science Reviews*. https://doi.org/10.1016/j.quascirev.2008.09.005

Roland, T. P., Caseldine, C. J., Charman, D. J., Turney, C. S. M., & Amesbury, M. J. (2014). Was there a "4.2ka event" in Great Britain and Ireland? Evidence from the peatland record. *Quaternary Science Reviews*, *83*, 11–27. https://doi.org/10.1016/j.quascirev.2013.10.024

Rosenberry, D. O., & LaBaugh, J. W. (2008). *Field Techniques for Estimating Water Fluxes Between Surface Water and Ground Water*. https://doi.org/10.3133/tm4D2

Scuderi, L. A., Yang, X., Ascoli, S. E., & Li, H. (2019). The 4.2 ka BP Event in northeastern China: A geospatial perspective. *Climate of the Past*, *15*(1), 367–375. https://doi.org/10.5194/cp-15-367-2019

Shapley, M. D., Ito, E., & Donovan, J. J. (2005). Authigenic calcium carbonate flux in groundwater-controlled lakes: Implications for lacustrine paleoclimate records. *Geochimica et Cosmochimica Acta*, *69*(10), 2517–2533. https://doi.org/10.1016/j.gca.2004.12.001

Shapley, Mark D., Ito, E., & Donovan, J. J. (2008). Isotopic evolution and climate paleorecords: Modeling boundary effects in groundwater-dominated lakes. *Journal of Paleolimnology*, *39*(1), 17–33. https://doi.org/10.1007/s10933-007-9092-3

Shinker, J. J. (2010). Visualizing spatial heterogeneity of western U.S. climate variability. *Earth Interactions*,

14(10). https://doi.org/10.1175/2010EI323.1

Shuman, B., Henderson, A. K., Colman, S. M., Stone, J. R., Fritz, S. C., Stevens, L. R., et al. (2009). Holocene lake-level trends in the Rocky Mountains, U.S.A. *Quaternary Science Reviews*, *28*(19–20), 1861–1879. https://doi.org/10.1016/j.quascirev.2009.03.003

Shuman, B., Pribyl, P., Minckley, T. A., & Shinker, J. J. (2010). Rapid hydrologic shifts and prolonged droughts in Rocky Mountain headwaters during the Holocene. *Geophysical Research Letters*. https://doi.org/10.1029/2009GL042196

Shuman, B. N., & Burrell, S. A. (2017). Centennial to millennial hydroclimatic fluctuations in the humid northeast United States during the Holocene. *Quaternary Research (United States)*, *88*(3), 514–524. https://doi.org/10.1017/qua.2017.62

Shuman, B. N., Carter, G. E., Hougardy, D. D., Powers, K., & Shinker, J. J. (2014). A north-south moisture dipole at multi-century scales in the Central and Southern Rocky Mountains, U.S.A., during the late Holocene. *Rocky Mountain Geology*, *49*(1), 33–49. https://doi.org/10.2113/gsrocky.49.1.33

Shuman, B. N., Pribyl, P., & Buettner, J. (2015). Hydrologic changes in Colorado during the mid-Holocene and Younger Dryas. *Quaternary Research (United States)*, *84*(2), 187–199. https://doi.org/10.1016/j.yqres.2015.07.004

Shuman, B. N., Marsicek, J., Oswald, W. W., & Foster, D. R. (2019). Predictable hydrological and ecological responses to Holocene North Atlantic variability. *Proceedings of the National Academy of Sciences of the United States of America*, *116*(13), 5985–5990. https://doi.org/10.1073/pnas.1814307116

Steinman, B. A., & Abbott, M. B. (2013). Isotopic and hydrologic responses of small, closed lakes to climate variability: Hydroclimate reconstructions from lake sediment oxygen isotope records and mass balance models. *Geochimica et Cosmochimica Acta*. https://doi.org/10.1016/j.gca.2012.11.027

Steinman, B. A., Abbott, M. B., Nelson, D. B., Stansell, N. D., Finney, B. P., Bain, D. J., & Rosenmeier, M. F. (2012). Isotopic and hydrologic responses of small, closed lakes to climate variability: Comparison of measured and modeled lake level and sediment core oxygen isotope records. *Geochimica et Cosmochimica Acta*, *105*, 455–471. https://doi.org/10.1016/j.gca.2012.11.026

Stewart, R. B., & Rouse, W. R. (1976). A Simple Method for Determining the Evaporation From Shallow Lakes and Ponds. *Water Resources Research*, *12*(4), 623–628. https://doi.org/10.1029/WR012i004p00623

795 Stokes, S., & Gaylord, D. R. (1993). Optical Dating of Holocene Dune Sands in the Ferris Dune Field, Wyoming.
796 *Quaternary Research*, *39*, 274–281.
797 Talbot, M. R. (1990). A review of the palaeohydrological interpretation of carbon and oxygen isotpic rations in
798 pimary lacustrine carbonates. *Chemical Geology (Isotope Geosci. Sect.)*, *80*, 261–279.
799 Talbot, M. R., & Kelts, K. (1990). Paleolimnological signatures from carbon and oxygen isotopic ratios in
800 carbonates from organic-rich lacustrine sediments. *Lacustrine Exploration: Case Studies and Modern*
801 *Analogs*, 99–112.
802 Tan, L. C., An, Z. S., Cai, Y. J., & Long, H. (2008). Hydrological representation of the 4.2 ka BP event in
803 China and its global linkages. *Geological Review*, *54*(1), 94-104.
804 Thompson, R. S., Whitlock, C., Bartlein, P. J., Harrison, S. P., Geoffrey Spaulding, W. (1993). Climatic Changes in
805 the Western United States since 18,000 yr B.P. In P. J. Wright, Jr., H. E., Kutzbach, J. E., Webb III, T.,
806 Ruddiman, W. F., Street-Perrott, F. A., Bartlein (Ed.), *Global Climates since the Last Glacial Maximum* (pp.
807 468–513). University of Minnesota Press.
808 Tyler, J. J., Leng, M. J., & Arrowsmith, C. (2007). Seasonality and the isotope hydrology of Lochnagar, a Scottish
809 mountain lake: Implications for palaeoclimate research. *Holocene*, *17*(6), 717–727.
810 https://doi.org/10.1177/0959683607080513
811 Walker, M., Gibbard, P., Head, M. J., Berkelhammer, M., Björck, S., Cheng, H., et al. (2019). Formal Subdivision
812 of the Holocene Series/Epoch: A Summary. *Journal of the Geological Society of India*, *93*(2), 135–141.
813 https://doi.org/10.1007/s12594-019-1141-9
814 Wang, Y., Cheng, H., Edwards, R. L., He, Y., Kong, X., An, Z., ... & Li, X. (2005). The Holocene Asian monsoon:
815 links to solar changes and North Atlantic climate. *Science*, *308*(5723), 854-857.
816 Wanner, H., Wanner, H., Mercolli, L., Mercolli, L., Grosjean, M., Grosjean, M., & Ritz, S. P. (2015). Holocene
817 climate variability and change; a data-based review. *Journal of the Geological Society*, *172*(2), 254–263.
818 https://doi.org/10.1144/jgs2013-101
819 Wanner, Heinz, Beer, J., Bütikofer, J., Crowley, T. J., Cubasch, U., Flückiger, J., et al. (2008). Mid- to Late
820 Holocene climate change: an overview. *Quaternary Science Reviews*, *27*(19–20), 1791–1828.
821 https://doi.org/10.1016/j.quascirev.2008.06.013
822 Wanner, Heinz, Solomina, O., Grosjean, M., Ritz, S. P., & Jetel, M. (2011). Structure and origin of Holocene cold

events. *Quaternary Science Reviews*, *30*(21–22), 3109–3123. https://doi.org/10.1016/j.quascirev.2011.07.010

Weiss, H. (2016). Climate change and cultural evolution across the world. *Past Global Change Magazine*, *24*(2), 62–63. https://doi.org/10.22498/pages.24.2.55

Weiss, H. (2019). Interactive comment on " Is there evidence for a 4 . 2 ka BP event in the northern North Atlantic region ?" by Raymond Bradley and Jostein Bakke. *Climate of the Past Discussions*. https://doi.org/https://doi.org/10.5194/cp-2018-162-RC2, 2019

Whitlock, C., & Bartlein, P. J. (1993). Spatial Variations of Holocene Climatic Change in the Yellowstone Region. *Quaternary Research*, *39*, 231–238.

Wise, E. K. (2010). Spatiotemporal variability of the precipitation dipole transition zone in the western United States. *Geophysical Research Letters*, *37*(7), n/a-n/a. https://doi.org/10.1029/2009gl042193

Xiao, J., Zhang, S., Fan, J., Wen, R., Zhai, D., Tian, Z., & Jiang, D. (2018). The 4.2 ka BP event: Multi-proxy records from a closed lake in the northern margin of the East Asian summer monsoon. *Climate of the Past*, *14*(10), 1417–1425. https://doi.org/10.5194/cp-14-1417-2018

Yan, M., & Liu, J. (2019). Physical processes of cooling and mega-drought during the 4.2 ka BP event: Results from TraCE-21ka simulations. *Climate of the Past*, *15*(1), 265–277. https://doi.org/10.5194/cp-15-265-2019

Zhang, H., Cheng, H., Cai, Y., Spötl, C., Kathayat, G., Sinha, A., et al. (2018). Hydroclimatic variations in southeastern China during the 4.2 ka event reflected by stalagmite records. *Climate of the Past*, *14*(11), 1805–1817. https://doi.org/10.5194/cp-14-1805-2018

Zhu, C., Lettenmaier, D. P., & Cavazos, T. (2005). Role of antecedent land surface conditions on North American monsoon rainfall variability. *Journal of Climate*, 18(16), 3104-3121. https://doi.org/10.1175/JCLI3387.1